

IOWA STATE UNIVERSITY
Digital Repository

Aerospace Engineering Publications

Aerospace Engineering

11-2016

Helical modes in boundary layer transition

Rikhi Bose

Iowa State University

Paul A. Durbin

Iowa State University, durbin@iastate.edu

Follow this and additional works at: http://lib.dr.iastate.edu/aere_pubs



Part of the [Aerodynamics and Fluid Mechanics Commons](#)

The complete bibliographic information for this item can be found at http://lib.dr.iastate.edu/aere_pubs/102. For information on how to cite this item, please visit <http://lib.dr.iastate.edu/howtocite.html>.

This Article is brought to you for free and open access by the Aerospace Engineering at Iowa State University Digital Repository. It has been accepted for inclusion in Aerospace Engineering Publications by an authorized administrator of Iowa State University Digital Repository. For more information, please contact digirep@iastate.edu.

Helical modes in boundary layer transition

Abstract

Observations are presented to show that in an adverse pressure gradient boundary layer, beneath free-stream turbulence, the interaction between Klebanoff streaks and naturally arising instability waves leads to helical disturbances which break down to form turbulent spots. This occurs under low to moderate levels, 1%–2%, of free-stream turbulence. At high levels of free-stream turbulence, conventional bypass mechanisms are seen.

The helical structures are clearly identifiable in visualizations of isosurfaces of streamwise perturbation velocity. A direct numerical simulation also was performed in zero pressure gradient, with a time-periodic Tollmien-Schlichting wave eigenfunction at the inlet. Again, under a moderate level of free-stream turbulence, helices were observed, and found to trigger transition. Their wave speed is on the order of $12U_\infty$, so helical breakdown can be viewed as a type of inner mode, secondary instability.

Disciplines

Aerodynamics and Fluid Mechanics | Aerospace Engineering

Comments

This article is published as Bose, Rikhi, and Paul A. Durbin. "Helical modes in boundary layer transition." *Physical Review Fluids* 1, no. 7 (2016): 073602. [10.1103/PhysRevFluids.1.073602](https://doi.org/10.1103/PhysRevFluids.1.073602). Posted with permission.

Helical modes in boundary layer transition

Rikhi Bose^{*} and Paul A. Durbin[†]

Department of Aerospace Engineering, Iowa State University, Ames, Iowa 50011, USA

(Received 29 August 2016; published 7 November 2016)

Observations are presented to show that in an adverse pressure gradient boundary layer, beneath free-stream turbulence, the interaction between Klebanoff streaks and naturally arising instability waves leads to helical disturbances which break down to form turbulent spots. This occurs under low to moderate levels, 1%–2%, of free-stream turbulence. At high levels of free-stream turbulence, conventional bypass mechanisms are seen. The helical structures are clearly identifiable in visualizations of isosurfaces of streamwise perturbation velocity. A direct numerical simulation also was performed in zero pressure gradient, with a time-periodic Tollmien-Schlichting wave eigenfunction at the inlet. Again, under a moderate level of free-stream turbulence, helices were observed, and found to trigger transition. Their wave speed is on the order of $\frac{1}{2}U_\infty$, so helical breakdown can be viewed as a type of inner mode, secondary instability.

DOI: [10.1103/PhysRevFluids.1.073602](https://doi.org/10.1103/PhysRevFluids.1.073602)

I. INTRODUCTION

Although boundary layer transition is usually considered to follow either an orderly route or a bypass route, in some circumstances these two routes may interact. Their interaction has been studied by computer simulations in which both free-stream disturbances and a Tollmien-Schlichting (TS) wave were introduced at the inlet. Adverse pressure gradient boundary layers, in which the instability waves arise “spontaneously,” provided the motivation for such studies.

In adverse pressure gradient (APG), instability waves grow fast enough to potentially couple with the strong Klebanoff streaks that arise under free-stream turbulence. In this regime, the transition mechanism may be called *mixed mode*, being a combination of orderly transition via instability waves, and bypass transition via Klebanoff streaks. The present article reports a mechanism that was observed in the mixed mode regime: Helical, secondary instabilities were seen, and they led to breakdowns to turbulent spots.

Helical breakdown has not been identified previously, although there are cases of, apparent, mixed mode transition in the literature. Spectra measured in experiments with APG, with incident free-stream turbulence [1,2], provide evidence that spontaneously occurring TS waves are noticeably present. In those studies, the investigators speculated that instability waves participate in the transition process, and, in that sense, it is more complex than pure bypass transition.

Simulations of transition on a compressor blade showed naturally occurring instability waves in the APG region on the pressure side [3]. In the presence of free-stream turbulence, the instability waves were visible and transition appeared to be of mixed mode type. In this case instability waves were observed, even when the intensity of the free-stream turbulence was not low. Figures in Brinkerhoff and Yaras [4] and Nagarajan *et al.* [5] suggest that helical disturbances may have been present in other simulations of APG boundary layer flow.

II. DIRECT NUMERICAL SIMULATION

The observations reported herein are from direct numerical simulation (DNS). The simulation code is a semi-implicit, staggered grid, finite volume method with fractional time stepping. It has been

^{*}rikhi004@gmail.com

[†]durban@iastate.edu

used in similar transition studies and is well documented [6,7]. Both zero pressure gradient (ZPG) and adverse pressure gradient (APG) flows were simulated. Adversity in the pressure gradient was created by a curved upper boundary, where impermeability and free-slip conditions are imposed on the velocity field. The curvature of the upper wall was designed to obtain a power law, $U_\infty(x) = Kx^m$, downstream of the inflow. The exponent is related to the Hartree parameter by $m = \beta_H/(2 - \beta_H)$; in the simulations, $\beta_H = -0.14$. This method was successfully used in other, recent studies on the effects of adverse pressure gradient on bypass transition [8,9]. Velocity profiles for the base flow with APG are in very good agreement with the corresponding Falkner-Skan similarity solution.

A broadband spectrum of free-stream disturbances comprising continuous eigenmodes of the uncoupled, Orr-Sommerfeld (OS), and Squire operators was set as the inflow. This procedure for free-stream turbulence synthesis is well documented, and has been validated against experiment [6,10,11]. The perturbation velocity components obtained by this method are isotropic, and satisfy continuity and viscous boundary conditions. Their amplitudes were selected to follow a von Karman energy spectrum.

Free-stream turbulence intensities $Tu \equiv [\frac{1}{3}(\bar{u}^2 + \bar{v}^2 + \bar{w}^2)]^{1/2}/U_\infty$ of 1% and 2% were used. The inlet Reynolds number in all simulations was $Re_b \equiv \sqrt{U_\infty x/v} = 398$, which corresponds to $R_\theta = 264$ for a Blasius profile. The length of the computational domain was $320\delta_0$, where δ_0 is the inlet 99% boundary layer thickness. The streamwise domain extends well beyond the upper branch of the zero pressure gradient neutral stability curve. The domain was wide enough ($20\delta_0$ in APG) so that imposed spanwise periodicity does not affect the flow. The grid resolution was better than the bypass transition simulations of Jacobs and Durbin [11].

III. HELICAL SECONDARY MODES IN ADVERSE PRESSURE GRADIENT

It has been shown in experiments and DNS that free-stream turbulence induces *low frequency Klebanoff streaks*. Mean shear prevents high frequency free-stream perturbations from penetrating the boundary layer [12]. Only low frequency components penetrate, and they amplify into strong, jetlike disturbances called (among other names) Klebanoff streaks.

Adverse pressure gradient boundary layers are inviscidly unstable. Instability waves are seen in numerical simulations, even in the absence of inlet disturbances [13]. The same was seen in the present geometry. However, their amplitude is low enough that transition does not occur in the present domain, without sufficient free-stream turbulence. At moderate Tu, as in the present simulations, transition to turbulence progresses through a mixed mode route. At high Tu it becomes pure bypass, with little role played by the instability waves. Laboratory experiments on transitional APG boundary layers under various levels of free-stream turbulence also provide evidence that different transition mechanisms are at play under moderate and high levels of Tu [1].

Contours of the wall normal component of the perturbation velocity (v'), in the horizontal x - z plane, are shown in Fig. 1 for both $Tu = 2\%$ and 1% —a solution with $Tu = 0\%$ is included, to show the natural instability wave. These are at a wall normal height $y = \delta_0/2$. For $Tu = 1\%$, a wavy pattern, that approximately crosses the whole span, is noticeable from $x = 140$ onward. These are primary instability waves, superimposed on the streaky, laminar base flow. They arise spontaneously within the simulation domain, as demonstrated in the lowest panel of Fig. 1. The phase speed of these discrete waves is similar to TS waves, $c \sim 0.36U_\infty$. A fast Fourier transform (FFT) of the v' component for the $Tu = 1\%$ case reveals the excited frequency to be approximately $0.17U_\infty/\delta_0$. The excited frequency does not match the frequency with the highest growth rate from linear theory, which is $0.135U_\infty/\delta_0$. However, that is to be expected, as the instantaneous base flow is distorted by Klebanoff streaks.

In Fig. 2(a), isosurfaces of streamwise perturbation velocity $u' = -0.085$ have been plotted. A streamwise wavy pattern is clearly visible. Here and in most figures, the waviness of interest occurs on *negative* streaks, $u' < 0$. In Fig. 2(b), u' contours are shown in the y - z plane at $x = 155$. A

HELICAL MODES IN BOUNDARY LAYER TRANSITION

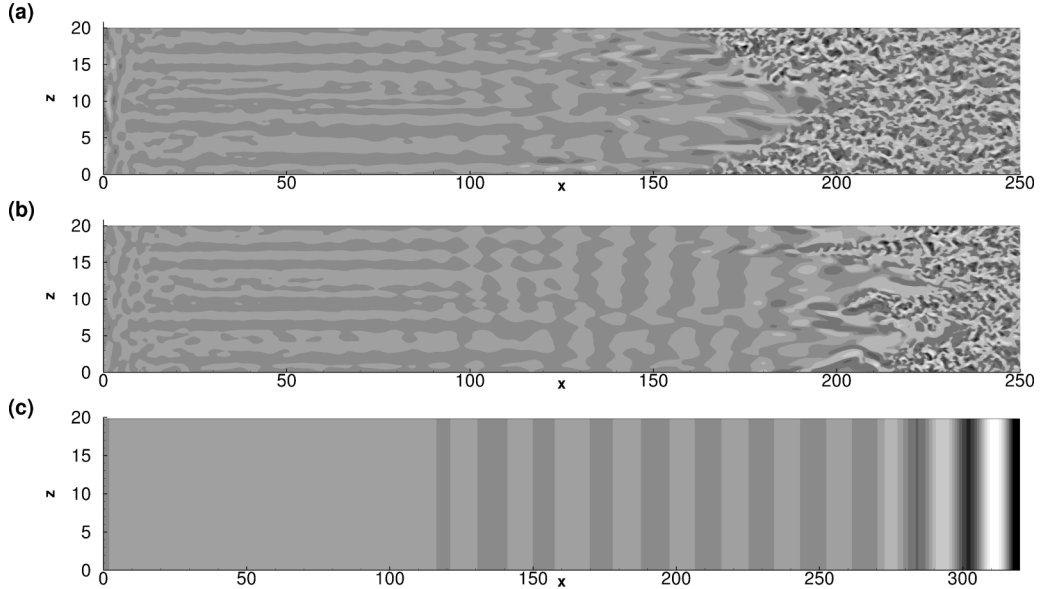


FIG. 1. $-0.2 \leq v' \leq 0.2$ contours in a horizontal x - z plane at $y = \delta_0/2$ for (a) $Tu = 2\%$ and (b) $Tu = 1\%$. (c) Contours of $-0.001 \leq u' \leq 0.001$ for $Tu = 0\%$ is shown for comparison.

positive streak is seen to glide over a negative streak, enhancing the shear at their junction. That is where the secondary instability initiates.

In the 1% case, it is especially apparent that the waviness is due to helical breakdown. Figure 3 is a frame from an animation. It illustrates several helical breakdowns upon contours of $u' = -0.085$. These develop into local, turbulent spots. This mechanism has not been recognized previously, but it appears to be evident in Brinkerhoff and Yaras's Fig. 16 [4].

The high-speed and low-speed Klebanoff streaks may be envisaged as jets or wakes in background shear. The helical instabilities might be imagined as developing on an approximately round wake; this is just for conceptual purposes, since the flow is not axisymmetric. For axisymmetric wakes and jets, normal mode components are written as [14]

$$[u_x, u_r, u_\phi] = [\hat{u}_x(r), \hat{u}_r(r), \hat{u}_\phi(r)] e^{ik_x(x-ct)+in\phi}.$$

Here, the integer value of $n = 0$ gives a toroidal mode while $n \neq 0$ are helical modes. A superposition of modes also may appear, as they are linear eigensolutions. Batchelor and Gill [14] showed that, for

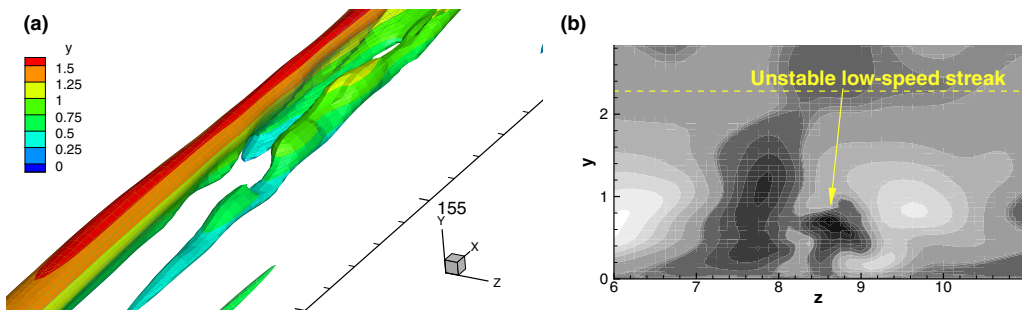


FIG. 2. (a) Isosurfaces of $u' = -0.085$ color contoured by wall distance y for $Tu = 2\%$ depicting a helical mode prior to turbulent spot formation. (b) $-0.25 \leq u' \leq 0.25$ contours in a wall normal y - z plane at $x = 155$. The boundary layer thickness at $x = 155$ is $\delta_{99} = 2.28\delta_0$.

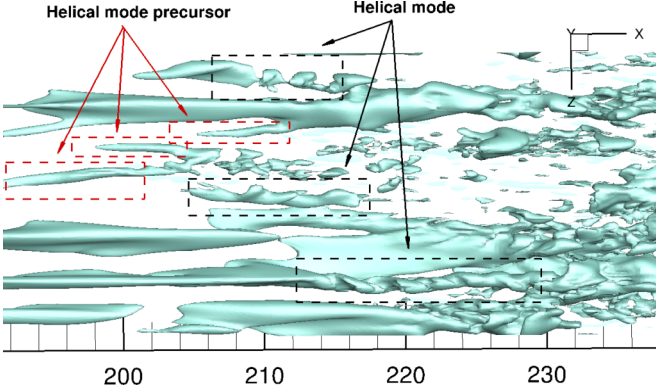


FIG. 3. Isosurfaces of $u' = -0.1$ showing several helical breakdowns for $Tu = 1\%$ within black boxes. Precursors that later become helical modes are also shown in red boxes.

smooth jet profiles, only $n = 1$ modes are inviscidly unstable. Michalke [15] found that the critical Reynolds number for $n = 0$ is always greater than that for $n = 1$, indicating that $n = 1$ modes are always more dangerous.

Helical features are seen both at $Tu = 1\%$ and 2% , but more frequently identifiable at $Tu = 1\%$. In Fig. 4(a), the onset of the helical $n = 1$ mode is shown by isosurfaces of $u' = -0.15$. The helical mode is fully formed in Fig. 4(b). It develops on a negative streak, in the high shear region between adjacent positive and negative streaks, as is shown in Fig. 4(c). Figure 4(d) shows u' contours in the

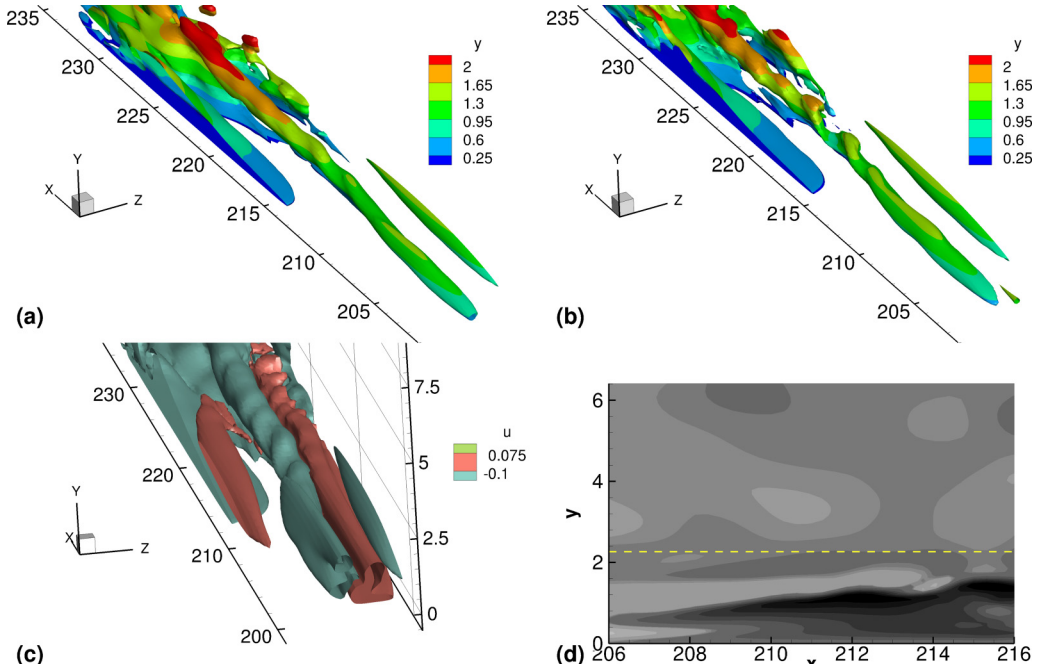


FIG. 4. (a) Isosurfaces of $u' = -0.15$ color contoured by wall distance y for $Tu = 1\%$ depicting a precursor to the helical mode. (b) Helical mode prior to turbulent spot formation. (c) Isosurfaces of u' showing the high shear region between high- and low-speed streaks at the same instant as (a). (d) $-0.3 \leq u' \leq 0.3$ contours in a wall normal $x-y$ plane cutting through the spot precursor in (a). The boundary layer thickness at $x = 215$ is $\delta_{99} = 2.26\delta_0$.

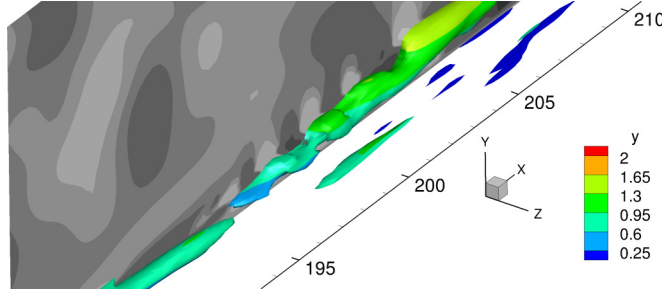


FIG. 5. A helical mode visualized by plotting isosurfaces of $u' = -0.1$ color contoured by wall distance y for $Tu = 1\%$; $-0.2 \leq v' \leq 0.2$ contours in the wall normal x - y plane cutting through the spot precursor is also shown. The boundary layer thickness at $x = 200$ is $\delta_{99} = 2.2\delta_0$.

x - y plane passing through the overlap region of these positive and negative streaks. The negative contours are dark. That the helical mode develops close to the wall is indicated by the dashed line marking $\delta_{99}(x)$. Hack and Zaki [6] found that inner modes develop in similar high shear regions. Contour plots of perturbation velocities in x - y planes passing through the high shear region between positive and negative streaks have the appearance of Kelvin-Helmholtz instability waves, as in free-shear flows. The overlapping surfaces are, of course, three dimensional (3D) and much more intricate. The 3D appearance is of a helical mode, being generated in the high shear between a pair of complicated, 3D, overlapping layers [16].

In Fig. 5, isosurfaces of $u' = -0.1$ have been plotted to show another helical disturbance. The $n = 1$ mode is readily recognizable. The figure also includes v' contours plotted in an x - y plane passing through the helix. At the chosen time instant, the helical mode at a given streamwise location has an azimuthal phase of, say, $\phi = \pi/2$ (the topmost, wall normal position of the mode). From the v' contours, it may be noted that the darkest contour (indicating the most negative v') lies in a region in between $\phi = -\pi/2$ (the bottom-most position of the isosurface plot) and $\phi = \pi/2$. Thus, the phase lag between u' and v' components is $\Delta\phi = \pi/2$. The continuity equation imposes an inherent phase difference of $\pi/2$ between the orthogonal components of a normal mode. Hence these are analogous to linear stability modes.

The phase speed of the helical modes was estimated as about 0.545 of the free-stream speed. This is consistent with the inner mode phase speeds obtained from a linear analysis by Vaughan and Zaki [17]. Also, the critical layer of these modes is close to the wall. For example, the helical mode shown in Fig. 5 has its critical layer at $y/\delta_{99} = 0.4$. However, the streamwise wavelength of helical modes is shorter than found by Vaughan and Zaki [17] for their inner modes. We found it to be around $1.0\text{--}1.3\delta_{99}$, while theirs was $2.85\delta_0$. So our observations fit with the inner mode framework, but are distinct from the solutions in Vaughan and Zaki.

Nagarajan *et al.* [5] simulated boundary layer transition with an inflow situated upstream of either a slender or a blunt leading edge. The C_p plots for the blunt leading edge had a strong APG region, before the elliptical leading edge merged with a flat section. For their blunt edge case, Nagarajan *et al.* noted the appearance of “wave packets” in the APG section, similar to Fig. 2. These led to breakdown. In Fig. 6, a horizontal plane cutting through the nascent turbulent spot in Fig. 2 is shown at a wall normal height $y = \delta_{99}/4$, where δ_{99} is the boundary layer thickness at $x = 155$. In the right column, the same perturbation components are shown from Nagarajan *et al.* [5]. Both are plotted at the same y/δ .

The contour plots show very good agreement with the present simulations at $Tu = 2\%$ for all three perturbation components. The plots from Nagarajan *et al.* [5] have a signature that is consistent with that of a helical mode. The w' component shows an antisymmetric pattern in the z direction. The v' contours are consecutively positive and negative and these lobes are inclined with respect to the x direction, as in helical modes (in the z region between 8.5 and 10 in the left column and

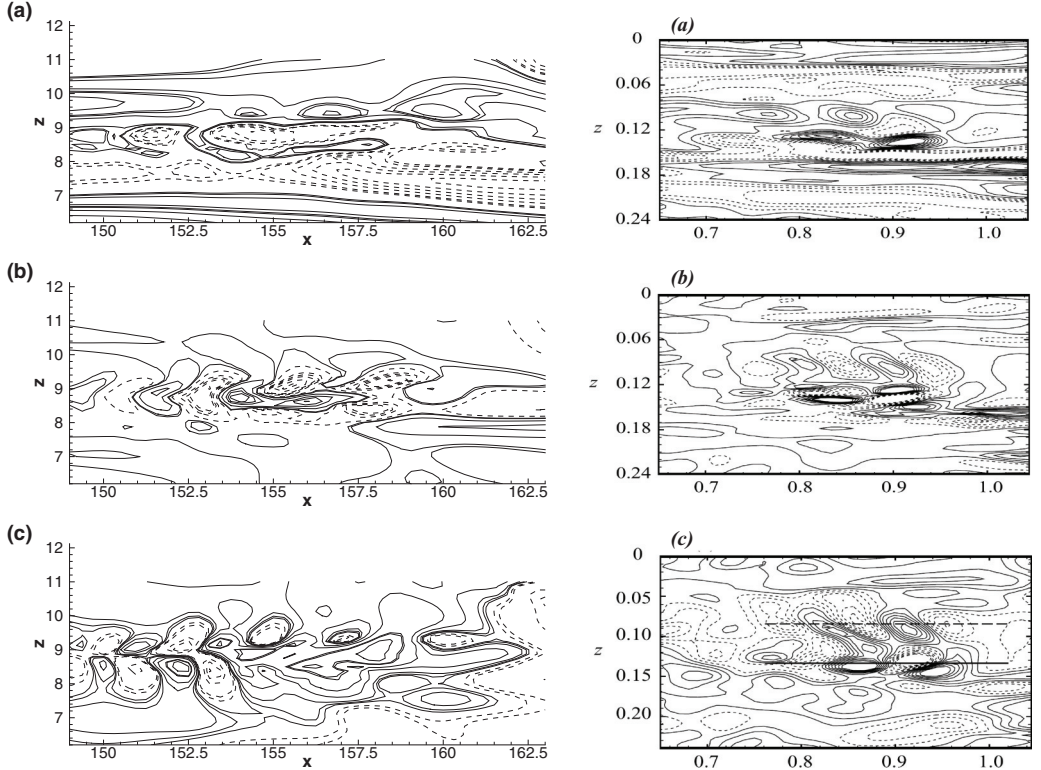


FIG. 6. x - z plane at wall distance $y = 0.25\delta_{99}$ cutting through the nascent turbulent spot shown in Fig. 2 in the left column compared to Nagarajan *et al.* [5] in the right column. (a) u' ; (b) v' ; (c) w' . Solid lines represent positive values.

between 0.06 and 0.12 in the right column). The u' contours in the left and right columns also show similar positive and negative lobes.

Figure 7 provides an additional view. u' isosurfaces are plotted over v' contours, at various wall normal distances. Dark is negative. The top frame corresponds to Fig. 6. There are maxima and minima of v' on the flanks of the u' isosurface, with a streamwise variation at the same wavelength as u' . These lobes are inclined. The minima below the u' isosurface correspond to a spiral that goes in, and on the other side, the maxima to where it comes out, of the plane. Half of the positive v' contour is under the isosurface, where it becomes $u' < 0$. In animations, this pattern breaks down quickly into a turbulent spot.

Distinction from outer instability

Helical mode breakdown is quite distinct from mechanisms seen in pure bypass transition. In ZPG, bypass transition is dominated by breakdown of low frequency, low-speed Klebanoff streaks, close to the edge of the boundary layer. Due to the higher critical layer and phase speed, this is designated as an *outer* instability by Vaughan and Zaki [17]. Visualizations have led to this being referred to as sinuous breakdown [6,10].

Figure 8 is an example. Perturbation velocity contours are plotted in a horizontal x - z plane at a wall normal height $y = \delta_0/2$. The yellow dashed box encloses the signature of an outer sinuous mode. The waviness is approximately planar. Spanwise antisymmetry in u' and v' and symmetry in w' is evident from Fig. 8. The contours of all three components replicate the pattern of outer eigenfunctions obtained from streak stability analysis (see Fig. 7 in Ref. [6]). The streamwise

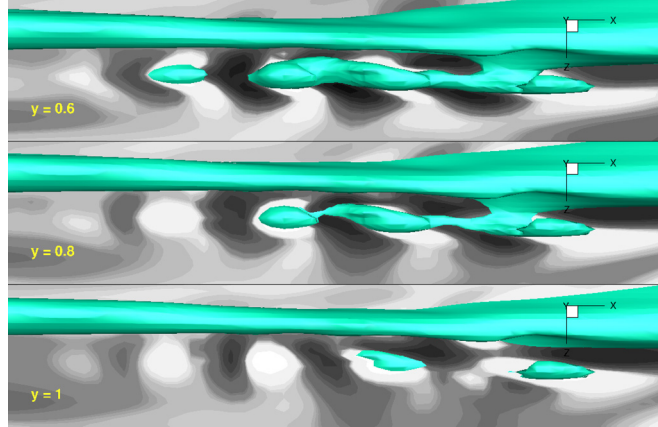


FIG. 7. u' isosurface and v' contours at different wall normal heights with respect to boundary layer thickness. Dark is negative. The top frame corresponds to Fig. 6.

wavelength of these modes is significantly larger than the helical modes. The phase speed is close to U_∞ , which is twice that of the helices.

In APG we did not observe outer instability with $Tu = 1\%$. With $Tu = 2\%$, a few instances of outer sinuous streak instability were noted in visualizations of the perturbation field.

IV. ZPG SIMULATIONS

It appears that helical secondary instability arises through the interaction of instability waves with Klebanoff streaks. Helical modes are *inner* instabilities. In recent literature on streak instability it has

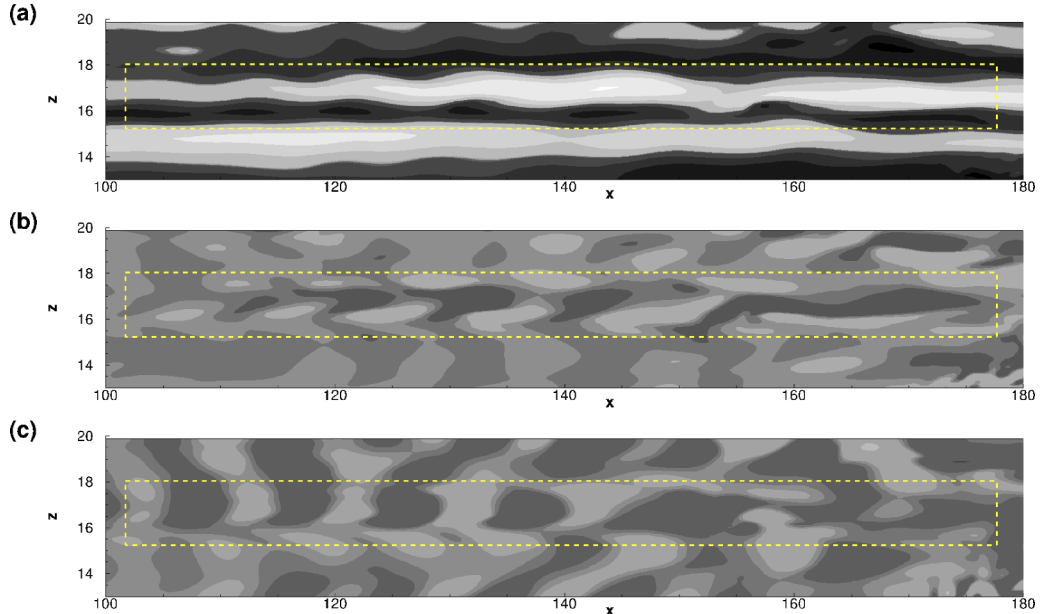


FIG. 8. Components of perturbation velocity in the horizontal x - z plane at a wall normal height $y = \delta_0/2$ for $Tu = 2\%$: (a) $-0.3 \leq u' \leq 0.3$; (b) $-0.15 \leq v' \leq 0.15$; (c) $-0.2 \leq w' \leq 0.2$. The scaling in the spanwise z direction has been enlarged twofold.

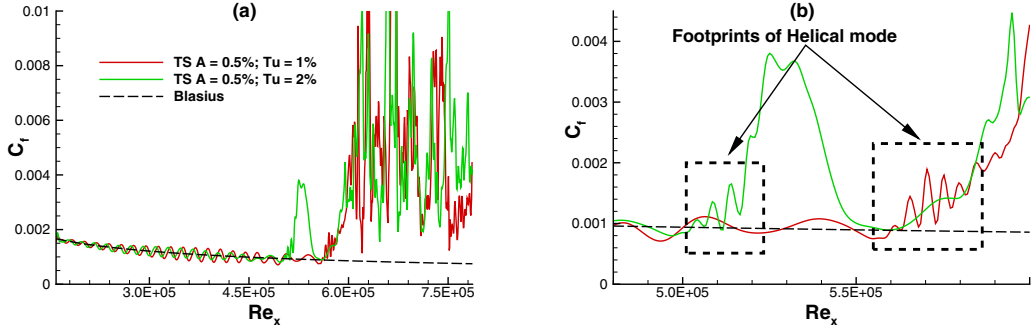


FIG. 9. Instantaneous, spanwise localized skin-friction coefficients (C_f) as functions of Re_x : (a) TS amplitude $A = 0.5\%$ and $Tu = 1\%$ or 2% at the inlet. (b) Zoomed in view of the C_f curves in (a). The wall normal plane of the plot passes through the helical modes.

been reported that the inner modes are expected to be more common in APG. The most pronounced effect of APG is an inflectional velocity profile, increasing the growth rate of instability waves. Is the inflectional base profile the underlying cause of the helical modes? If so, then the helical modes should not be seen in ZPG, even in the presence of TS waves. Or is a mode interaction the trigger?

To empirically answer these questions, as a fundamental study, TS instability waves were introduced along with free-stream turbulence into a ZPG domain. If the TS amplitude is large, the situation studied by Liu *et al.* [18] is recovered, in which streaks distort the TS wave to create horseshoe vortices. For present purposes the amplitude is lower.

The inflow profile had a time-periodic TS wave eigenfunction and free-stream turbulence superimposed on the Blasius profile. The TS wave is unstable at the Reynolds number $Re_b = 400$. Its nondimensional frequency is $F \equiv 10^6 \omega v / U_\infty^2 = 124$. Its amplitude at the inlet is 0.5% of U_∞ . The intensity of free-stream turbulence remained the same as the APG simulations. The conditions are similar to those of Liu *et al.* [18] but with a lower TS wave amplitude.

Almost all the breakdowns observed at $Tu = 1\%$ were by helical modes. At $Tu = 2\%$, some breakdowns were triggered by the helical, inner instability, while in others, sinuous, outer instability was the dominant mode. In Fig. 9(a), instantaneous C_f has been plotted for both Tu cases along a constant z line passing through the helical modes. The TS wave grows and starts decaying prior to breakdown. Hence, transition occurs after the upper branch. Figure 9(b) is a zoomed in view: the footprints of helices show streamwise wavy structure (as was also seen in Ref. [5]).

In Fig. 10(a), isosurfaces of $u' = -0.15$ have been plotted for the $Tu = 1\%$ case. The helical instability is clearly identifiable. The development of the streaks and emergence of the helix are very similar to the $Tu = 1\%$, APG case—which does not have any TS wave provided at the inlet.

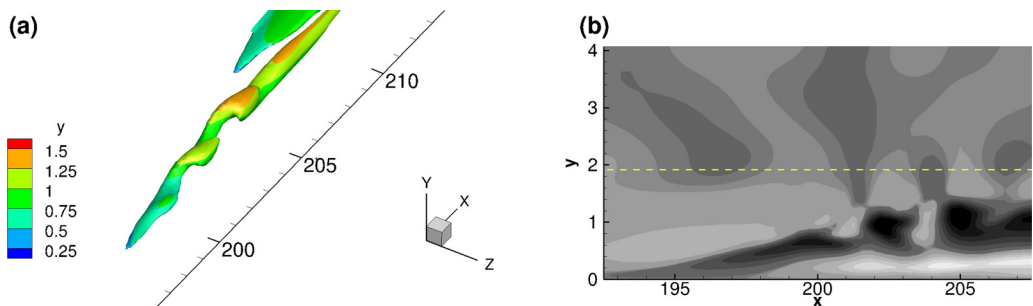


FIG. 10. (a) Isosurfaces of $u' = -0.15$ color contoured by wall distance y for $TS\ A = 0.5\%$ and $Tu = 1\%$ depicting the helical mode. (b) $-0.25 \leq u' \leq 0.25$ contours in the x - y plane passing through the spot. At $x = 205$, $\delta_{99} = 1.92\delta_0$.

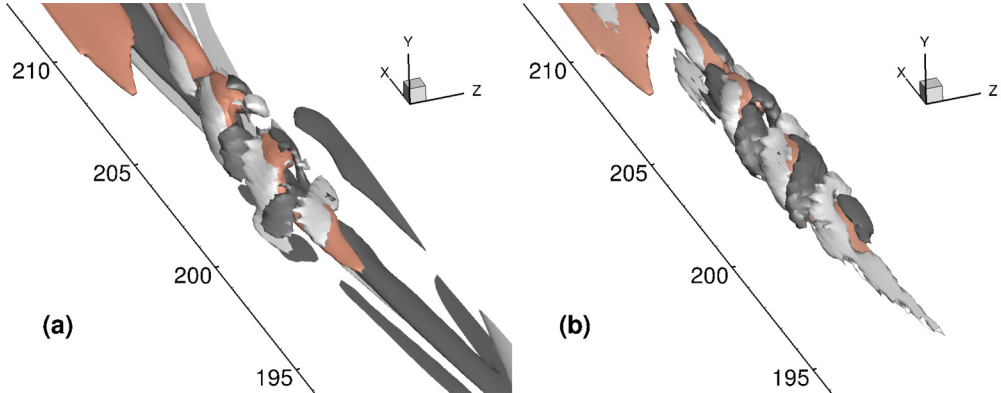


FIG. 11. (a) Isosurfaces of $u' = -0.15$ for the helical mode shown in Fig. 10. Isosurfaces of streamwise vorticity are also shown for $\omega_x = +0.2$ (gray) and $\omega_x = -0.2$ (white). (b) Isosurfaces of streamwise vorticity tilting term $T = +0.05$ (gray) and $T = -0.05$ (white) at the same instant as (a).

In Fig. 10(b), u' contours are plotted in the x - y plane passing through the helix. The instability takes place well inside the boundary layer. Again, it originates in the high shear at the overlap of a high-speed streak and a low-speed streak. The phase speed, streamwise wavelength, and critical layer are the same as those of the helical modes seen in APG.

The streaks are jetlike, streamwise perturbations; these may be termed the primary perturbations. The helices are flow structures observed in u' isosurfaces. Therefore, these may be termed secondary perturbations. Decomposition of the instantaneous streamwise vorticity component (ω_x) in the following manner helps identify these secondary perturbations [6]:

$$\omega_x = \bar{\omega}_x + \omega_x^p + \omega_x^s.$$

Here, $\bar{\omega}_x = 0$ for the mean flow. $\omega_x^p \approx 0$, as the streaks are primarily in u' . Therefore, $\omega_x \approx \omega_x^s$, where ω_x^s denotes the streamwise vorticity due to secondary perturbations.

Isosurfaces of ω_x for a pair of positive and negative values have been plotted in Fig. 11(a), at the same instant as in Fig. 10, along with the isosurfaces of $u' = -0.15$ depicting the helical mode. Prior to the formation of the helical mode, isosurfaces of ω_x wrap around the unstable streak. After the genesis of the helical mode, the isosurfaces of ω_x also orient in an approximately helical pattern. For $x > 200$, troughs and crests in ω_x become apparent along the helical structure. The isosurfaces of ω_x wrap around the isosurfaces of u' .

In the transport equation for ω_x , the tilting term is $T = \omega_y \frac{\partial U}{\partial y} + \omega_z \frac{\partial U}{\partial z}$. (As initially ω_x is weak and the streamwise gradient of U is small, the tilting term is larger than the stretching term.) In Fig. 11(b), instantaneous isosurfaces of $T = \pm 0.05$ have been plotted. Clearly, the isosurfaces are very nicely correlated with the helical mode, indicating that the secondary perturbations are of vortical nature. The positive component wraps around the negative part of u' and maintains a phase difference of π in the azimuthal direction with the negative component, in a given plane.

To demonstrate that the helical structure is not an artifice of shading or lighting effects of the plotting software, contours are plotted in cross-sectional planes. Figure 12(a) shows several wall normal planes, slicing through a helical structure. Contours of negative u' have been plotted in these planes in Fig. 12(b). The contour levels have been selected so that the shift of the minima may be followed, in successive downstream planes. The wall normal planes have been numbered in both plots, to correspond. In Fig. 12(a), the contours plotted in Fig. 12(b) are shown to wrap around the structure. The locus of the minimum shifts from lower y , in plane 1, to a higher y in section 4. While doing so, it also shifts continuously, first leftward, then rightward, to ultimately finish at approximately the same spanwise location in plane 4 as in plane 1. One notices a similar development

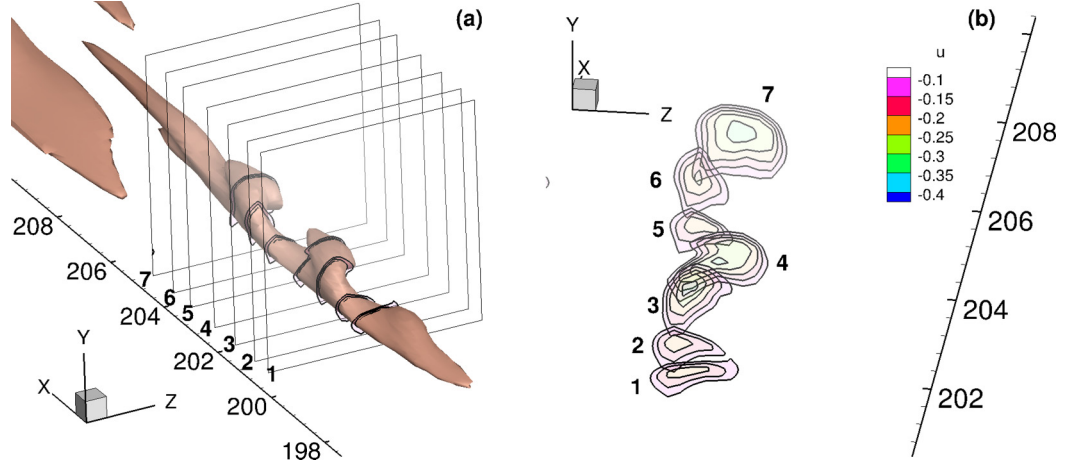


FIG. 12. (a) Isosurfaces of $u' = -0.15$ showing the helical mode. Seven wall normal planes at selected streamwise stations that are numbered are chosen which slice through the helical mode. The locations where these planes cut through the helices are also marked. (b) Contours of $u' < 0$ in the seven wall normal planes shown in (a) show the clear helical pattern of the mode.

from plane 4 to plane 7. Thus, the cross sections show that the structure is indeed helical, and not an artifice of the visualization method.

Figure 13 illustrates both that helices occur commonly, and that they break down into patches of turbulence. These are frames from an animation. Both left and right handed helices occur. Their wavelengths are quite shorter than the TS wave.

The mode interaction simulations in ZPG show that the inner, helical modes are not due to an inflectional base flow, *per se*. The main elements appear to be a moderate OS discrete mode amplitude and moderate Tu. The former arises naturally in APG. The latter is a criterion that bypass transition by outer mode instability is not predominant. Perhaps helical breakdown may be designated as a mechanism that lies between orderly (low Tu high TS) and bypass (high Tu) when instability waves are present.

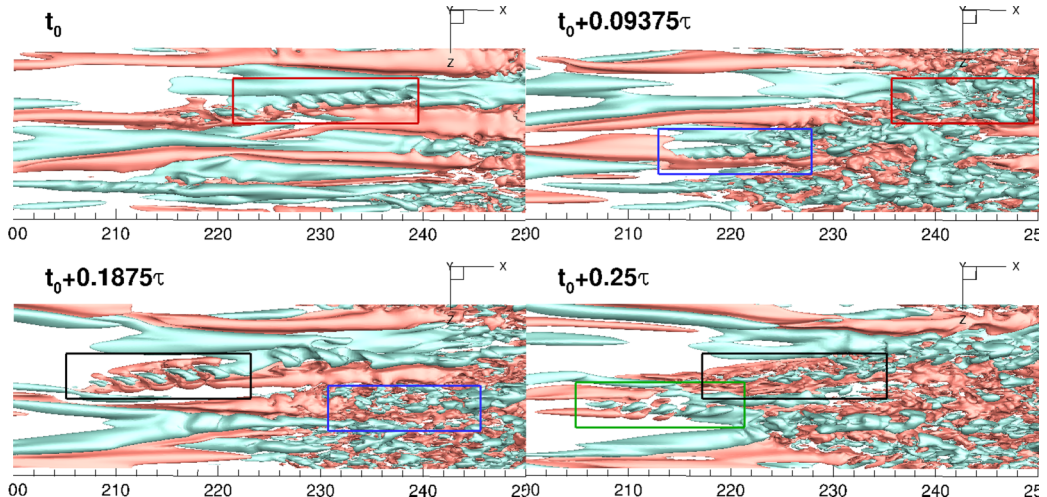


FIG. 13. Evolution of helices into turbulence. Blue $u' = -0.1$; red, $u' = 0.1$. The boxes encircle helices and the patch of turbulence they spawn. Here, τ denotes one flow through time.

V. CONCLUSION

The purpose of this article is to report observations of a new type of boundary layer transition. It arises through the interaction of Klebanoff streaks and instability waves. Instability waves on the base flow are excited spontaneously in APG boundary layers. Beneath free-stream turbulence, the turbulence intensity dictates the transition route. The streak amplitude, *per se*, does not seem to dictate whether helical or outer sinuous modes dominate.

For $Tu \lesssim 2\%$, helical breakdown is observed on low-speed streaks. The phase speed and critical layer indicate that the helical modes should be classified as inner instabilities [17]. At higher $Tu (> 2\%)$, the helical modes breakdown before becoming fully developed. Outer sinuous instabilities also trigger breakdown at this level. At even higher Tu , conventional bypass mechanisms prevail.

While the evidence presented herein indicates that helices form when instability waves and Klebanoff modes interact, we have no theoretical explanation. The helical wavelength is shorter than the TS instability wave, and has no apparent relation to it. TS waves have their critical layer near the wall, as do the helical waves. Liu *et al.* [18] attributed the interaction of higher amplitude TS waves and streaks to a resonant instability, which they analyzed by Floquet theory. It is conceivable that the helices can be attributed to a resonant interaction as well.

ACKNOWLEDGMENTS

This work was supported by National Science Foundation (NSF) Grant No. CBET-1228195. Computer time was provided by the Extreme Science and Engineering Discovery Environment (XSEDE), which is supported by NSF Grant No. ACI-1053575 [19]. Discussion with Prof. Tamer Zaki is greatly appreciated.

- [1] J. P. Gostelow, A. R. Blunden, and G. J. Walker, Effects of free-stream turbulence and adverse pressure gradients on boundary layer transition, *J. Turbomach.* **116**, 392 (1994).
- [2] G. J. Walker and J. P. Gostelow, Effects of adverse pressure gradients on the nature and length of boundary layer transition, *J. Turbomach.* **112**, 196 (1989).
- [3] T. Zaki, J. Wissink, W. Rodi, and P. Durbin, Direct numerical simulations of transition in a compressor cascade: The influence of free-stream turbulence, *J. Fluid Mech.* **665**, 57 (2010).
- [4] J. R. Brinkerhoff and M. I. Yaras, Numerical investigation of transition in a boundary layer subjected to favourable and adverse streamwise pressure gradients and elevated free stream turbulence, *J. Fluid Mech.* **781**, 52 (2015).
- [5] S. Nagarajan, S. K. Lele, and J. H. Ferziger, Leading-edge effects in bypass transition, *J. Fluid Mech.* **572**, 471 (2007).
- [6] M. J. P. Hack and T. A. Zaki, Streak instabilities in boundary layers beneath free-stream turbulence, *J. Fluid Mech.* **741**, 280 (2014).
- [7] X. Wu, R. G. Jacobs, P. A. Durbin, and J. Hunt, Simulation of boundary layer transition induced by periodically passing wakes, *J. Fluid Mech.* **398**, 109 (1999).
- [8] K. P. Nolan and T. A. Zaki, Conditional sampling of transitional boundary layers in pressure gradients, *J. Fluid Mech.* **728**, 306 (2013).
- [9] T. Zaki and P. A. Durbin, Continuous mode transition and the effects of pressure gradient, *J. Fluid Mech.* **563**, 357 (2006).
- [10] L. Brandt, P. Schlatter, and D. S. Henningson, Transition in boundary layers subject to free-stream turbulence, *J. Fluid Mech.* **517**, 167 (2004).
- [11] R. G. Jacobs and P. A. Durbin, Simulations of bypass transition, *J. Fluid Mech.* **428**, 185 (2001).
- [12] J. C. R. Hunt and P. A. Durbin, Perturbed vortical layers and shear sheltering, *Fluid Dyn. Res.* **24**, 375 (1999).

- [13] S. Lardeau, M. Leschziner, and T. Zaki, Large eddy simulation of transitional separated flow over a flat plate and a compressor blade, *Flow, Turbul. Combust.* **88**, 19 (2012).
- [14] G. K. Batchelor and A. E. Gill, Analysis of the stability of axisymmetric jets, *J. Fluid Mech.* **14**, 529 (1962).
- [15] A. Michalke, Survey on jet instability theory, *Prog. Aerospace Sci.* **21**, 159 (1984).
- [16] L. Brandt and H. C. de Lange, Streak interactions and breakdown in boundary layer flows, *Phys. Fluids* **20**, 024107 (2008).
- [17] N. J. Vaughan and T. A. Zaki, Stability of zero-pressure-gradient boundary layer distorted by unsteady Klebanoff streaks, *J. Fluid Mech.* **681**, 116 (2011).
- [18] Y. Liu, T. A. Zaki, and P. A. Durbin, Boundary-layer transition by interaction of discrete and continuous modes, *J. Fluid Mech.* **604**, 199 (2008).
- [19] J. Towns, T. Cockerill, M. Dahan, I. Foster, K. Gaither, A. Grimshaw, V. Hazlewood, S. Lathrop, D. Lifka, G. D. Peterson, R. Roskies, J. R. Scott and N. Wilkins-Diehr, XSEDE: Accelerating Scientific Discovery, *Comput. Sci Eng.* **16**, 62 (2014).